



MINIMUM ATTENUATION GUARANTEED BY AN ACTIVE NOISE CONTROL SYSTEM IN PRESENCE OF ERRORS IN THE SPATIAL DISTRIBUTION OF THE PRIMARY FIELD

V. MARTIN AND C. GRONIER

*Laboratoire de Mécanique de Rouen, UPRESA CNRS 6104, INSA de Rouen,
Avenue de l'Université, BP08, 76801 Saint Etienne du Rouvray Cedex, France*

(Received 21 July 1997, and in final form 5 June 1998)

The optimal attenuation of sound fields inside moving vehicles in cruise conditions by active acoustic control depends on the number and locations of acoustic secondary sources. When taking measurements is difficult or expensive, as in airplanes, launchers etc., the best number and locations can be determined, on the one hand, from harmonic numerical modelling to obtain the interior vibro-acoustic responses inside the vehicles, and on the other hand by the help of a calculated map providing the spatial distribution of the primary excitation. It turns out that the predicted attenuations are always optimistic when compared with the measured attenuation while the numerical response functions and the primary field correspond quite well to those measured. From among the reasons for the discrepancy, one is analyzed in the present paper: a numerical frequency model works with a perfectly stationary primary field in space, which is not the case in the real world. Indeed, the spatial distribution of the primary field always varies around a central one called here the primary field of reference. In these conditions, the present study shows the gap between the minimum attenuation guaranteed by a control system and the optimal attenuation associated with the primary field of reference. This gap increases with the latter reference attenuation. The study also gives the attenuation which a numerical model should provide in the reference situation in order to guarantee a minimum attenuation when knowing the errors in the spatial distribution of the primary field. This new information is of great importance for calculations carried out to predict the efficiency of active control of harmonic sound fields.

© 1998 Academic Press

INTRODUCTION

The active acoustic control of an unwanted sound field, called the primary field, consists of driving loudspeakers by a particular signal in order to radiate permanently a field with the same amplitude and with opposite phase throughout the domain considered, so that each field will cancel the other out to result in a reduction of the primary sound level. The two scientific aspects of active control

lie in the spatial reconstruction of a sound field at each moment, and in the temporal synchronicity at each point. The precise synchronicity at one point was the aim of past research.

When the goal is to control an entire domain, the state of the art is very different. Even by considering signals which are elementary in time, such as sinusoids, the precise reconstruction of a given acoustic field in an entire domain is unachievable due to the practical impossibility for a secondary source to be installed where the unwanted known source is, or due to the practical impossibility for a finite number of secondary sources to radiate a predetermined field (Kirchhoff–Helmholtz theorem). By limiting ourselves to such elementary signals, i.e., to harmonic sound fields, the improvement of the control performance in an entire domain necessitates that at least two major difficulties be overcome: that of reconstructing at best a perfectly stationary field in space with the help of a secondary source configuration (and with well-located sensors); and that of guaranteeing that an efficient geometrical configuration of sources is still efficient when the sound field varies in space, in the sense that both its amplitude and phase vary in space as time goes by.

In fact, the objective of spatial acoustic reconstruction is usually reached only in a mean-square sense with a small number of secondary sources making an attempt to reduce the unwanted sound field at a large number of points in the domain considered. Numerous source configurations exist which differ in their number and locations of sources. Each configuration has its own capacity for reducing the sound level and, until now, they have been classified by the optimal attenuation they make possible. To achieve this, the classification has been made by using particular strategies to choose the sources [1] or with natural methods [2], or by optimizing the source locations for each configuration [3].

The optimal attenuation for each source configuration is calculated from the frequency responses of the sources at the control microphones and from the primary field measured at the same microphones. Most of the time, the primary field is not known precisely and the classification of the configurations by the sole criterion of the reference optimal attenuation, i.e., with the optimal attenuation of a given primary field, also said of the reference, may no longer be adequate. Tacitly it is expected that the most efficient configurations are also those of greatest “solidity” to primary field variations. This point constitutes the subject of the present paper, upon bearing in mind predictive studies with numerical modelling of the acoustic domain considered, often coupled with a vibrating structure.

For a given frequency, suppose that a numerical model is available and describes perfectly the acousto-structural behavior of a vehicle, allowing one to be confident about all the response functions between sources and points inside the acoustic domain, these points playing the role of microphones. A harmonic reference primary field made up of acoustic pressures inside the vehicle the complex amplitude $p_{in}(x)$ is provided by measurements taken by the manufacturer who also knows, say by experience, the dispersion of the field around its mean value. The mean field is the reference field, and the dispersion is said to be known through $e_{in} = \|\delta p_{in}\|_{L^2} / \|p_{in}\|_{L^2}$ where the L^2 -norm is made up of the summation over a large

number of points in the acoustic domain. The present problem consists in finding the configurations of secondary acoustic sources, chosen from among a significant number N_{max} of predetermined locations, which ought to be efficient—in respect to the optimal attenuation achievable—and resistant to primary field variations; i.e., which are still able to give good attenuation even if the primary field is no longer the one with which the source number and locations were obtained. In other words, it is asked of the configuration to guarantee a good minimum attenuation.

The same goal has to be reached in a slightly different situation extracted from a problem investigated in the past [4]. Upon still supposing a perfect numerical model built for a given frequency, which describes the passengers' cabin of a propeller-driven aircraft, realistic calculated maps of the external pressure applied to the fuselage exist and constitute the external excitation of the numerical model. Measuring the external pressure everywhere on the fuselage in flight is impossible. At best, one could hope to carry out a small number of measurements at a few points and to determine the ratio $e_{ex} = \|\delta p_{ex}\|_{L^2} / \|p_{ex}\|_{L^2}$ where the L^2 -norm has now to be understood as the summation over the small number of measured points. With the hypothesis that this ratio is valid for what happens on the whole external side of the fuselage, the linearity of the model leads to $e_{in} = \|\delta p_{in}\|_{L^2} / \|p_{in}\|_{L^2}$. Indeed $p_{in} = K p_{ex}$ where K is the matrix of the model and p_{ex} the excitation. It follows that $\|\delta p_{in}\|_{L^2} \leq \|K\|_{L^2} \|\delta p_{ex}\|_{L^2}$ and e_{in} . Here also, the problem consists in finding the configuration which satisfies criteria of efficiency and of resistance to primary field variations with its correlate regarding the guaranteed minimum optimal attenuation.

This paper first describes the approximated theoretical aspects concerning both the acoustic attenuation and the resistance of a secondary source configuration to primary field variations. It is emphasized again that the work is carried out for harmonic sound fields, the amplitudes and phases of which vary in space. The notion of relative variation of the primary field will be developed throughout the text.

Secondly, one consequence of the approximated theoretical description ought to have been that the greater the optimal reference attenuation, the smaller the minimum guaranteed attenuation. In fact, numerical simulations with very elementary calculations allow one to determine the validity limit of the theoretical result obtained at this stage.

The great interest of what has been observed concerning the results of the simple numerical simulations justifies the effort made to find and, now to provide, the demonstration of the closed form of the minimum guaranteed attenuation.

To show that, in fact, the attenuations are always higher than the minimum attenuation calculated, active control experiments are carried out in the simplest way; i.e., with one or two primary sources, two microphones and one control-source.

Finally, it will be noted that the discrepancy between optimal and minimum guaranteed attenuations is of the same magnitude as the gap between those predicted with a numerical model excited by a perfectly spatially-stationary primary field and the attenuations effectively measured *in situ*.

2. APPROXIMATED THEORETICAL APPROACH TO SOURCE CONFIGURATION SOLIDITY AND DISCUSSION OF ITS VALIDITY

2.1. ACOUSTIC LEVEL AND ATTENUATION

An acoustic source radiates an acoustic pressure, written as $p(x, t)$ to emphasize its dependence on space and time. When the pressure has the very particular form $p(x, t) = a(x) \cos(2\pi ft + \gamma(x))$, i.e., the pressure is a pure tone periodic in time with frequency f , with amplitude a and phase γ depending on x only, the acoustic pressure is expressed as a real part of a complex quantity: $p(x, t) = \Re(a(x) e^{i\gamma(x)} e^{i\omega t})$ where $\omega = 2\pi f$ is the radian frequency. What is called the complex amplitude is made up of $a(x) e^{i\gamma(x)}$ and is also called the complex pressure $p(x)$ which does not take into account the time-dependence. Due to the linearity of the equation, the solution of which is such an acoustic pressure, the real part is omitted during calculations and inserted again only at the end of the calculations (some authors prefer to express the pressure as an imaginary part simply because they use the sine instead of the cosine). Moreover, the linearity makes it possible to forget the time term $e^{i\omega t}$ as the whole quantity will share the same time-dependence. In these conditions, the spatial problem is written in the complex field with the far simpler unknown $p(x)$. If the final solution has to be expressed as a function of space and time, the term $e^{i\omega t}$ has to recover its place before taking the real part of the global complex expression.

In the work presented here, the time dependence is $e^{i\omega t}$ since the frequency is fixed, but amplitude a and phase γ , both functions of x , are uncertain due to a lack of exact information, or by extension, due to a certain instationarity in time, but with a time-scale far greater than the period $T = 1/f$.

This paper will be concentrated on some effects caused by the difference between one acoustic pressure and another at the same place, and then on the effects of the square of the difference integrated or summed in space. For example, in space and time, quantities such as $\delta p(x, t) = (a(x) + \delta a(x)) \cos(\omega t + \gamma(x) + \delta\gamma(x)) - a(x) \cos(\omega t + \gamma(x))$ will be considered. The amplitude of $\delta p(x, t)$ results from both variations $\delta a(x)$ and $\delta\gamma(x)$. Indeed, with the simplest case of $\delta a(x) = 0$ but in presence of $\delta\gamma(x)$, $\delta p(x, t) = 2a(x) \sin(\delta\gamma(x)/2) \sin(\omega t - (\delta\gamma(x)/2))$, leading to the amplitude of $\delta p(x, t)$ being $2a(x) \sin(\delta\gamma(x)/2)$ (this can be seen by developing δp as above and using usual trigonometric relations, or the well-known geometrical representation of Fresnel). Of course, taking the square of the pressure variation and integrating it over space will result in a quantity, written $\|\delta p\|_{L^2}^2$, depending on the variations of both amplitude and phase.

A primary source radiates a harmonic sound pressure field $p_0(x)$: i.e., made up of the complex amplitude of the pressure at each point x of a domain. When the number of points x is finite, the pressure can be described by a vector \mathbf{p}_0 made up of as many components as observation points x , the values of which therefore depend on x . The sum of the squares of the absolute values of the pressure in the present context. This can be called the global sound level— $J^p = \mathbf{p}_0^* \cdot \mathbf{p}_0$ (* denotes the transpose conjugate). This latter quantity is associated with the acoustic potential energy.

Indeed, the definition of the acoustic potential energy in a domain Ω is $U(t) = -(1/2) \int_{\Omega} p(x, t) \operatorname{div} \mathbf{u}(x, t) dx$ where p and \mathbf{u} are respectively the acoustic pressure and displacement. The conservation of mass associated with the equation of state of a perfect adiabatic gas, written at the first order (in linear acoustics) is $p = -\rho c^2 \operatorname{div} \mathbf{u}$ where ρ and c are the gas density and the sound speed in the gas, and results in $U(t) = (1/2\rho c^2) \int_{\Omega} p^2(x, t) dx$. When entering into the frequency domain, i.e., for time dependence $e^{i\omega t}$ in the complex field (see, e.g., reference [5]), the potential energy is given by $U(\omega) = (1/2\rho c^2) \int_{\Omega} \bar{p}(x)p(x) dx$. If the domain Ω is discretized by a finite number of points x_i , the discretized form of the integral gives $U(\omega) = (\Delta x_i/2\rho c^2) \sum_i \bar{p}(x_i)p(x_i)$ with Δx_i being the area associated with point x_i (of course, as long as Δx_i is a constant). Had J^p been multiplied by the term $\Delta x_i/2\rho c^2$, it would have had the exact form of the discretized acoustic potential energy associated with the primary field \mathbf{p}_0 . To go further, writing $J^p = \mathbf{p}_0^* \cdot \mathbf{p}_0$ in the form of $\|\mathbf{p}_0\|_{L^2}^2$, the L^2 -norm takes on the sense of a physical energy as it is derived from the acoustic potential energy.

Let $g(x, x_s)$ be the harmonic response at a point x of a unit excitation applied at a source situated at point x_s . The set of responses at a certain number of points from various sources is gathered in the matrix \mathbf{G} , called the transfer matrix or frequency response matrix, the components of which depend on x and x_s . The driving signals applied to the secondary sources at x_s , constitute the vector Φ .

With the secondary sources on, the total pressure is the sum of the primary and secondary pressures. The global sound level is thus

$$J(\phi) = \|\mathbf{p}_0(x) + \mathbf{G}(x, x_s) \cdot \Phi\|_{L^2}^2 = \Phi^* \cdot \mathbf{H} \cdot \Phi + 2\Re(\Phi^* \cdot \Phi) + J^p. \quad (1)$$

The matrix $\mathbf{H} = \mathbf{G}^* \cdot \mathbf{G}$ is positive definite and is often called the matrix of secondary energy. The reason is that $\Phi^* \cdot \mathbf{H} \cdot \Phi = \mathbf{p}_s^* \cdot \mathbf{p}_s$ or $\|\mathbf{p}_s\|_{L^2}^2$ with \mathbf{p}_s the pressure radiated by the secondary sources. As already mentioned, the L^2 -norm is associated, here, with the potential energy of the secondary pressure. The physical sense of $\Phi = \mathbf{G}^* \cdot \mathbf{p}_0$ is not so easy to develop. Without going too far in this direction, we can at least say that it corresponds to the retropropagation of the primary field to the secondary sources.

The sound level is a quadratic function of the driving signal of the sources and the minimum of the function is reached when the driving signal, called the optimal control signal, depends linearly on the primary field in the following way:

$$\Phi_{opt} = -\mathbf{H}^{-1} \cdot \Phi = -\mathbf{H}^{-1} \cdot \mathbf{G}^* \cdot \mathbf{p}_0 = \mathbf{L} \cdot \mathbf{p}_0. \quad (2)$$

The rectangular matrix \mathbf{L} exhibits the linear relation.

The space spanned by the control vector can be given a norm such that $\|\Phi\|_H^2 = \Phi^* \cdot \mathbf{H} \cdot \Phi$ from which the sound level can be written as $J(\Phi) = \|\Phi - \Phi_{opt}\|_H^2 - \|\Phi_{opt}\|_H^2 + J^p$ and, in particular, the optimal residual sound level is

$$J_{min} = -\|\Phi_{opt}\|_H^2 + J^p = -\Phi^* \cdot \mathbf{H} \cdot \Phi + J^p = -\mathbf{p}_0^* \cdot \mathcal{A} \cdot \mathbf{p}_0 + J^p, \quad (3)$$

where $\mathcal{A} = \mathbf{G} \cdot \mathbf{H}^{-1} \cdot \mathbf{G}^*$ has the property $\mathcal{A}^2 = \mathcal{A}$ from which it is known that the eigenvalues are 0 or 1: i.e., $\|\mathcal{A}\|_{L^2} = 1$. If all eigenvalues of \mathcal{A} are 1, this means that \mathcal{A} is the identity matrix and thus that $J_{min} = 0$, in other words, \mathbf{p}_0 is totally

controllable. If all eigenvalues are 0, \mathbf{p}_0 is not controlled at all. It is thus clear that \mathcal{A} exhibits the part of the primary field which is controllable. It has been explicitly shown [6] that \mathcal{A} projects the primary field vector into the space of totally controllable pressures, a space which is built from the transfer matrix \mathbf{G} .

As for the optimal attenuation in dB, it is deduced from equation (3) and expressed by

$$A_0 = -10 \log_{10} \left(\frac{J_{min}}{J^p} \right) = -10 \log_{10}(1 - R_0) = -\frac{10}{\ln(10)} \ln(1 - R_0), \quad (4)$$

with $R_0 = \|\mathbf{p}_0\|_{\mathcal{A}}^2 / \|\mathbf{p}_0\|_{L^2}^2 = \|\Phi_{opt}\|_H^2 / \|\mathbf{p}_0\|_{L^2}^2$.

A_0 is called the optimal attenuation of the primary field \mathbf{p}_0 thanks to the secondary sources described by their transfer matrix \mathbf{G} . For the purposes of the present paper, A_0 will be called here the optimal attenuation of the primary field of reference \mathbf{p}_0 . As for R_0 , it can be seen to be the ratio of the secondary to the primary potential energy, according to the explanations given previously.

2.2. SOLIDITY OF THE OPTIMAL ATTENUATION WITH REGARD TO PRIMARY FIELD VARIATIONS

The first approach to the sensitivity presented here was given in a thesis done under the direction of the first author [7]. This section explores in greater depth that first approach and adds the notion of the guaranteed minimum attenuation, so fundamental for predictive studies, say by numerical modelling.

The acoustic attenuation is a real function of a complex variable, as R_0 is a real number on the interval $[0, 1]$ while \mathbf{p}_0 is a vector, the components of which are in the complex field. Throughout the development, the derivative of a real function f of a complex variable $x = a + ib$ is defined by $f_x = f_{,a} + if_{,b}$.

When the primary field is submitted to a variation $\delta\mathbf{p}_0$, the optimal attenuation is submitted to a variation, in the real field, $\delta A_0 = A_0(\mathbf{p}_0 + \delta\mathbf{p}_0) - A_0(\mathbf{p}_0)$. At the first order this variation is also $(\delta\mathbf{p}_0^R)' \cdot (\partial A_0 / \partial \mathbf{p}_0^R) + (\delta\mathbf{p}_0^I)' \cdot (\partial A_0 / \partial \mathbf{p}_0^I)$ where the superscripts R and I signify real and imaginary parts. With the above definition of the derivative, the Taylor series of A_0 at the first order is

$$\delta A_0 = \Re(\delta\mathbf{p}_0^* \cdot \partial A_0 / \partial \mathbf{p}_0) + O(\delta\mathbf{p}_0^* \cdot \delta\mathbf{p}_0). \quad (5)$$

The Schwartz inequality results in $|\delta A_0|^2 \leq \|\delta\mathbf{p}_0\|^2 \cdot \|\partial A_0 / \partial \mathbf{p}_0\|^2$ with the norm in L^2 .

The derivative of the optimal attenuation in respect to the primary field is

$$\frac{\partial A_0}{\partial \mathbf{p}_0} = +\frac{10}{\ln(10)} \frac{1}{1 - R_0} \frac{\partial R_0}{\partial \mathbf{p}_0}.$$

Let $R(\mathbf{p}) = (\mathbf{p}^* \cdot \mathcal{A} \cdot \mathbf{p}) / \|\mathbf{p}\|_{L^2}^2$ be the value of which is R_0 at \mathbf{p}_0 .

The definition of the derivative and the use of the property of \mathcal{A} lead to $\partial(\mathbf{p}^* \cdot \mathcal{A} \cdot \mathbf{p}) / \partial \mathbf{p} = 2\mathcal{A} \cdot \mathbf{p}$, and thus $\partial R / \partial \mathbf{p} = \{2(\mathbf{p}^* \cdot \mathbf{p})\mathcal{A} \cdot \mathbf{p} - 2(\mathbf{p}^* \cdot \mathcal{A} \cdot \mathbf{p})\mathbf{p} / \|\mathbf{p}\|_{L^2}^4$.

The sensitivity of the optimal attenuation A_0 to the primary field \mathbf{p}_0 is defined by:

$$\frac{\partial A_0}{\partial \mathbf{p}_0} = + \frac{20}{\ln(10)} \frac{1}{1 - R_0} \frac{\mathcal{A} \cdot \mathbf{p} - R_0 \mathbf{p}}{\|\mathbf{p}_0\|_{L^2}^2}, \tag{6}$$

and the square of its norm is

$$\left\| \frac{\partial A_0}{\partial \mathbf{p}_0} \right\|_{L^2}^2 = v^2 \frac{R_0}{1 - R_0} \frac{1}{\|\mathbf{p}_0\|_{L^2}^2},$$

which does not depend explicitly on \mathcal{A} , i.e., on the configuration of the physical system of control (made up of the secondary sources and the sensors).

Finally the Schwartz inequality applied to the Taylor series at the first order eventually bounded by an upper value $(\delta A)_{adm}$, which could be called the admissible attenuation variation, results in

$$|\delta A_0| \leq v \cdot e \cdot \sqrt{\frac{R_0}{1 - R_0}} = (\delta A)_{max} \leq (\delta A)_{adm}, \quad \text{with} \quad e = \frac{\|\delta \mathbf{p}_0\|_{L^2}}{\|\mathbf{p}_0\|_{L^2}}. \tag{7}$$

In other words, for a given value of e , and independently of the physical system of control, each optimal attenuation in the reference situation (for primary field \mathbf{p}_0) has its own maximum attenuation variation $(\delta A)_{max}$, or, for a given admissible attenuation variation $(\delta A)_{adm}$, there exists a value of the reference optimal attenuation which should not be exceeded.

At first sight, the lower the reference optimal attenuation A_0 (or its corresponding value R_0), the lower the maximum optimal attenuation variation $(\delta A)_{max}$: the most solid configuration is the one which gives the smallest reference optimal attenuation. In Figure 1, attenuation versus configurations is imagined. On the x -axis, secondary source configurations have been classified to allow their actual optimal attenuation to decrease towards the right-hand side. In these conditions, the smallest reference optimal attenuation would be on the black spot at the right extremity.

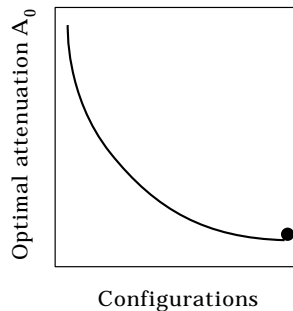


Figure 1. Imagined situation: secondary source configurations classified in order to show the optimal attenuation versus the configuration to be decreasing. The most solid configuration, at the black point, is the least efficient in the reference situation.

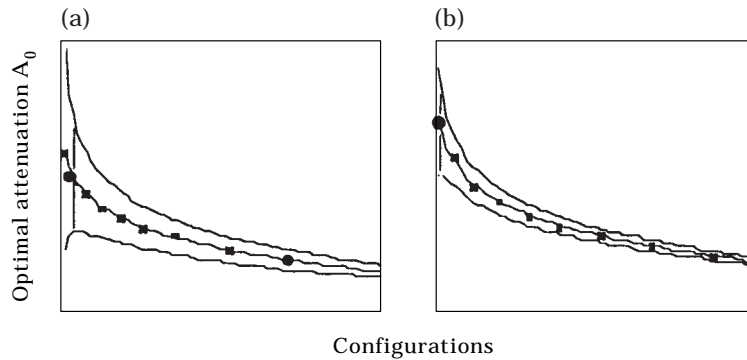


Figure 2. Imagined situation: secondary source configurations classified in order to show the optimal attenuation versus the configuration to be decreasing. (a) Case of a compromise between optimal attenuation and narrow corridor (black point); (b) case where the greatest attenuation remains advantageous as it ensures the greatest of the minimum attenuation guaranteed (black point).

What can be done when the smallest attenuation associated to R_0 is far too small to be kept? In Figure 2, secondary source configurations have also been classified for attenuation A_0 to decrease to the right. The same figure shows two imagined situations of the error corridor, made up of the domain between $A_0 - (\delta A)_{max}$ and $A_0 + (\delta A)_{max}$, that could occur as this stage. In case 2(a), the best optimal attenuation is not kept because the error corridor is too large; the smallest attenuation is not kept for it is far too small; a compromise is found at the second best attenuation (black spot). In case 2(b), the greatest attenuation remains interesting because it ensures the best of the minimum attenuations defined by $A_{min} = A_0 - (\delta A)_{max}$. It is thus essential to know when these situations are going to occur in the real world.

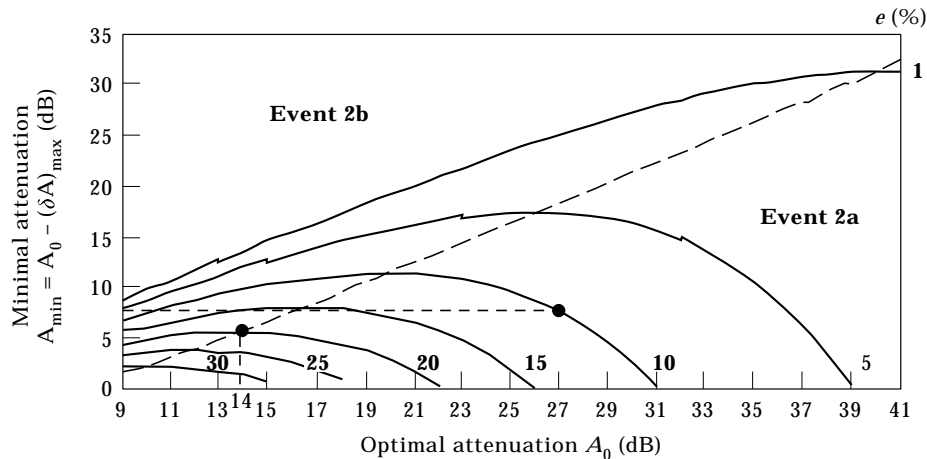


Figure 3. Graphs of the minimum attenuations guaranteed by the development at the first order of the Taylor series of the optimal attenuation against the primary field for various values of e (the black points correspond to special examples in the text).

The graph of $A_{min} = A_0 - (\delta A)_{max}$ as a function of the reference optimal attenuation A_0 for various values of e are drawn in Figure 3. These graphs indicate which configuration, with its optimal attenuation, leads to the best minimum attenuation. For example for $A_0 = 27$ dB and $e = 20\%$, no minimum attenuation can be guaranteed. But for $e = 10\%$, 27 dB of reference optimal attenuation can guarantee 8 dB. According to these graphs, with $e = 20\%$ the best policy is to seek an attenuation of 14 dB to guarantee 5 dB.

Now let a line be drawn joining the maximum minimum attenuations for each value of e . Above this line the configuration gives an optimal attenuation of type 2(b) where it is worthwhile to improve the reference attenuation as the minimal attenuation will also improve. On the contrary, below this line, the case is that of 2(a), where the increase in the attenuation is accompanied by a decrease in the minimal attenuation.

In fact, very simple calculations to simulate active control will show that situations 2(a) are probably impossible. It would have been impossible to envisage such calculations without the information provided in the present section.

2.3. REMARK CONCERNING RELATIVE ERROR e , INPUT OF THE PROBLEM

The present goal is to determine the minimum attenuation that can be guaranteed, given the optimal attenuation in the reference situation and given the relative error e of the primary field. Until now, the minimum attenuation has been defined by $A_{min} = A_0 - (\delta A)_{max}$ where $(\delta A)_{max}$ is the upper bound of δA_0 , provided the Taylor series at the first order is valid. The smaller the upper bound, the better the minimum attenuation guaranteed. As soon as A_0 (or R_0) and e are known, the die is cast concerning A_{min} .

The knowledge of e is a hypothesis. It has been assumed that a manufacturer could know the value of e . If this is true and if the value of e is quite small, say no more than 20%, the guaranteed minimum optimal attenuation will be obtained directly. On the contrary, if there is very little chance for e to be known by experience, it is always possible to take measurements of the primary field at a small number of points, to compare with the primary field of reference at the same points (obtained for example from a map calculated to predict this field) and to calculate the value of e from the small number of measurements. The next step consists in accepting that the value obtained is representative of what could have been calculated, had the measurements at a large number of points been possible. The hypothesis of the knowledge of e is replaced by that of the representativity of e calculated from a small number of measurements.

The latter procedure will allow a more precise definition of the value of e which has to enter into the definition of $(\delta A)_{max}$.

Indeed, first note that the optimal attenuation of the primary field \mathbf{p}_0 remains unchanged when this field is multiplied by a scalar, in other words: $A_0(\mathbf{p}_0) = A_0(\alpha \mathbf{p}_0)$, $\alpha \in \mathbb{C}$. The coefficient α will change the amplitude and phase of the vector \mathbf{p}_0 , changing in the same way the vector of the driving signal applied to the secondary source, but without any influence on the optimal attenuation. The

variation in the optimal attenuation resulting from a variation $\delta \mathbf{p}_0$ in the primary field can thus be written

$$\delta A_0 = |A_0(\mathbf{p}_0) - A_0(\mathbf{p}_0 + \delta \mathbf{p}_0)| = |A_0(\mathbf{p}_0) - A_0(\alpha(\mathbf{p}_0 + \delta \mathbf{p}_0))|, \quad (8)$$

leading to

$$\delta A \leq v \cdot e' \cdot \sqrt{\frac{R_0}{1 - R_0}} = v \cdot \frac{\|\mathbf{p}_0 - \alpha(\mathbf{p}_0 + \delta \mathbf{p}_0)\|_{L^2}}{\|\mathbf{p}_0\|_{L^2}} \cdot \sqrt{\frac{R_0}{1 - R_0}}, \quad (9)$$

where e' is a quadratic function of α and there exists a value of α which minimizes e' minimizing also the upper bound of δA_0 (and not δA_0 itself).

Since $\tilde{\mathbf{p}}_0 = \mathbf{p}_0 + \delta \mathbf{p}_0$ and $e' = \|\mathbf{p}_0 - \alpha \tilde{\mathbf{p}}_0\|_{L^2} / \|\mathbf{p}_0\|_{L^2}$, the minimization of e' through α results in $\alpha = (\tilde{\mathbf{p}}_0^* \cdot \mathbf{p}_0) / \|\tilde{\mathbf{p}}_0\|_{L^2}^2$, depending on the projection of \mathbf{p}_0 on $\tilde{\mathbf{p}}_0$ which is the spatial distribution of the primary acoustic field differing from the distribution of reference described by \mathbf{p}_0 . The minimal value e_{min} of e is

$$e_{min} = \frac{\left\| \mathbf{p}_0 - \frac{\tilde{\mathbf{p}}_0^* \cdot \mathbf{p}_0}{\|\tilde{\mathbf{p}}_0\|_{L^2}^2} \cdot \tilde{\mathbf{p}}_0 \right\|_{L^2}}{\|\mathbf{p}_0\|_{L^2}}. \quad (10)$$

This value is used during the following elementary calculations.

The reduction of $(\delta A)_{max}$ through the reduction of e in e_{min} has not yet been provided with a physical interpretation. It is, for the time being, a pure result of calculation.

2.4. ELEMENTARY CONTROL SIMULATION BY SIMPLE CALCULATIONS

The graph of the minimum optimal attenuation A_{min} versus the reference optimal attenuation A_0 and the error in spatial stationarity is now sought by another way consisting of very simple calculations which will have the great advantage over the first theoretical approach of not being restricted to the so-called first-order.

The very simple implementation rests on information originating from the previous paragraphs. Indeed one has first learned that the reference optimal attenuation of the “vector” \mathbf{p}_0 depends only on its direction and not on its norm, as $A_0(\mathbf{p}_0) = A_0(\alpha \mathbf{p}_0)$, $\forall \alpha \in \mathbb{C}$. Second, the Taylor series at the first order has indicated that $(\delta A)_{max}$ depends on e_{min} as defined in equation (10). Upon admitting momentarily that, for a given value of A_0 (or R_0), $(\delta A)_{max}$ depends on e_{min} whatever the order of the development, then $A_{min} = A_0 - (\delta A)_{max}$ would be a function of e_{min} only. The lack of information lies in the relation between A_{min} and A_0 without considering the primary field \mathbf{p}_0 and the physical control systems. This point will be clarified.

The simple calculation procedure is now given. From a few arbitrary primary fields \mathbf{p}_0 that are to be cancelled out at two or more microphones by one or more secondary acoustic sources, it is easy to obtain A_0 [see equations (1)–(4)] and then to let each \mathbf{p}_0 vary by a certain quantity $\delta \mathbf{p}_0$ to obtain the new optimal attenuation $A_0(\mathbf{p}_0 + \delta \mathbf{p}_0)$. Like the primary fields, the secondary fields defined by \mathbf{G} [see equation (1)] are totally arbitrary. A great number of such tests will provide the

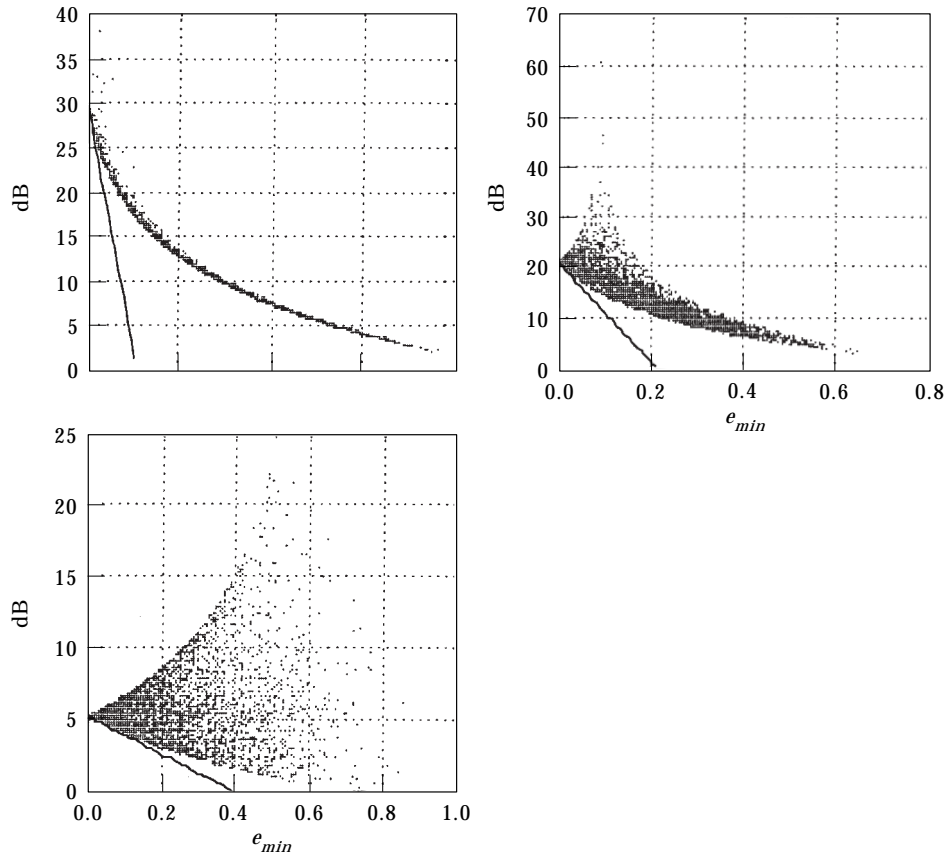


Figure 4. Possible optimal attenuations for primary fields far from a reference field of a value e_{min} (physical configuration made up of one secondary-source and two microphones). \square , Optimal attenuation; —, $A_0(\mathbf{p}_0) - \delta A_{max}$.

smallest optimal attenuation A_{min} against e_{min} starting with A_0 . Figure 4 shows, for a particular configuration made up of one control-source and two microphones, the results achieved. Some points should now be emphasized.

- (1) For the same value of e_{min} there exist several variations $\delta \mathbf{p}_0$ which lead to different optimal attenuations.
- (2) One can define $A_{max}(e_{min})$ as the maximum value of optimal attenuations reached for various primary fields $\tilde{\mathbf{p}}_0$ of given e_{min} ; $A_{max}(e_{min})$ begins by increasing and then decreases when e_{min} increases; of course, $A_{max} = A_0$ for $e_{min} = 0$; the graphs also show that at least one field $\tilde{\mathbf{p}}_0$ leads to an optimal attenuation A_0 of infinite value, which can be obtained by working on equation (3) by imposing $J_{min} = 0$.
- (3) One can define $A_{min}(e_{min})$ as the minimum value of optimal attenuations reached for various primary fields $\tilde{\mathbf{p}}_0$ of given e_{min} ; there exists a graph $A_{min}(e_{min})$ which decreases with great regularity when e_{min} increases; of course $A_{min} = A_0$ when $e_{min} = 0$.

For the same configuration of the physical control system, the same type of graphs are obtained from other values of A_0 . In these graphs, the lines $A_0 - (\delta A)_{max}$, where $(\delta A)_{max}$ is obtained by the Taylor series at the first order, are drawn. The discrepancy is vertiginous when A_0 and e_{min} are large.

The present simulations by using very simple calculations have shown that, effectively, A_{min} does not depend on the “vector” \mathbf{p}_0 at the origin of A_0 as several primary fields giving the same optimal attenuations lead to the same graphs. The dependence on the physical configuration does not seem to exist either as several physical configurations giving the same reference optimal attenuation also lead to the same graphs. In these conditions A_{min} depends on A_0 without considering \mathbf{p}_0 and the physical system of control.

The previous simulations make it possible to obtain the graph $A_{min}(A_0)$ according to e_{min} . Figure 5 shows the results. This figure originates from calculations and not from a demonstration, unlike Figure 3. It is reliable as no restrictive theoretical hypotheses exist, but it is not entirely satisfactory in the sense that it does not yet come from a demonstration.

In Figure 5 the squares, triangles and circles correspond, for a given e_{min} , to various configurations which reduce different primary fields. If one imagines a line going through the points, the graph so drawn depends solely on A_0 and not on \mathcal{A} : i.e., not on the physical configuration, nor on the primary field \mathbf{p}_0 at the origin of A_0 .

When e_{min} is 30%, it is quite clear that the minimum optimal attenuation starts to increase with the reference optimal attenuation and then reaches a kind of a plateau, the asymptotic value of which is around 10 dB (minimal attenuation). Effort to improve the reference attenuation beyond 20 dB will not be rewarded as the minimum guaranteed attenuation will not be improved to the same extent. On this curve corresponding to $e_{min} = 30\%$, the Taylor series at the first order would be useful only up to a reference attenuation of 4 dB!

At the other extremity, i.e., for very small values of e_{min} , for example for $e_{min} = 5\%$, the Taylor series is valid up to 20 dB of reference attenuation. For such values of e_{min} , it remains worthwhile to reach the best reference attenuation as the

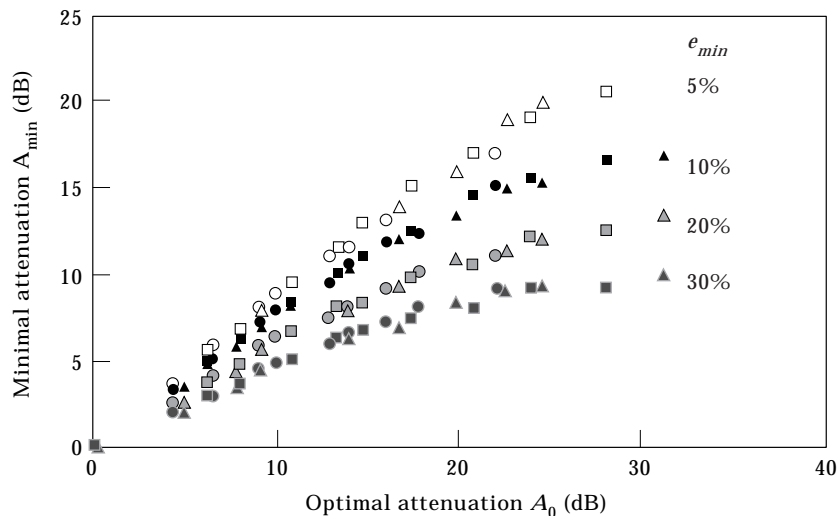


Figure 5. Graphs of the minimum guaranteed optimal attenuation against the reference optimal attenuation for various values of e_{min} . Obtained from graphs as in Figure 4.

minimal guaranteed attenuation will benefit. However the reader should note that for an error of 5%, 25 dB of minimum reduction requires 40 dB of reference attenuation.

3. CLOSED FORM OF THE MINIMUM GUARANTEED ATTENUATION

3.1. FORMULATION OF THE PROBLEM

This part of the paper will end with the closed form of the minimal attenuation which will occur given the reference primary field optimally attenuated by a source configuration and given the value of the minimized primary field relative error e_{min} . The demonstration is derived from the previous considerations.

The source configuration is written in the matrix form \mathcal{A} , and the optimal attenuation achievable for an arbitrary primary field \mathbf{p} (different from the reference primary field) is (see equation (4)):

$$A_0(\mathbf{p}) = -10 \log_{10} \left(1 - \frac{\mathbf{p}^* \cdot \mathcal{A} \cdot \mathbf{p}}{\|\mathbf{p}\|_{L^2}^2} \right) = -10 \log_{10} \left(\frac{\mathbf{p}^* \cdot \mathcal{K} \cdot \mathbf{p}}{\|\mathbf{p}\|_{L^2}^2} \right),$$

$$\text{with } \mathcal{K} = \mathbf{I} - \mathcal{A}.$$

\mathcal{A} and \mathcal{K} are projection matrices (their use for active control is developed in reference [6]). It should be remembered that there exists a set of primary fields, the optimal attenuation of which is the same (see Section 2.3): this set is composed of the fields where corresponding vectors are in the same direction whatever their amplitudes. It should also be remembered that there exists a set of fields \mathbf{p} which share the same value of e_{min} .

The problem consists in looking for the minimum value of A_0 under the constraint of a given value a of e_{min} . The programming is thus: find A_{min} such that

$$A_{min} = \min_p A_0(\mathbf{p}) \text{ with the property that } A_{min} = \min_{\pi = \alpha \mathbf{p}} A_0(\boldsymbol{\pi}) \forall \text{ the scalar } \alpha$$

$$e_{min}(\mathbf{p}) = \frac{\left\| \mathbf{p}_0 - \left(\frac{\mathbf{p}^* \cdot \mathbf{p}_0}{\|\mathbf{p}\|_{L^2}^2} \right) \mathbf{p} \right\|_{L^2}}{\|\mathbf{p}_0\|_{L^2}} = a, \text{ a quantity depending on } \mathbf{p} \text{ through}$$

$$h(\mathbf{p})\mathbf{p} = \left(\frac{\mathbf{p}^* \cdot \mathbf{p}_0}{\|\mathbf{p}\|_{L^2}^2} \right) \mathbf{p}, \tag{11}$$

where $h(p)$ corresponds to the projection of \mathbf{p}_0 on $\tilde{\mathbf{p}}$. Here $\boldsymbol{\pi}$ is an acoustic pressure field.

Due to the property of A_{min} , it is always possible to choose α arbitrarily and, for future technical reasons, the choice will be made so that $h(\mathbf{p})\mathbf{p}$ takes the form $\boldsymbol{\pi} = \alpha \mathbf{p}$. It results in $|\alpha^2|/\alpha^* = (\mathbf{p}^* \cdot \mathbf{p}_0)/\|\mathbf{p}\|_{L^2}^2$ or $1 = (\boldsymbol{\pi}^* \cdot \mathbf{p}_0)/\|\boldsymbol{\pi}\|_{L^2}^2$, leading to

$e_{min}(\boldsymbol{\pi}) = (\|\mathbf{p}_0 - \boldsymbol{\pi}\|_{L^2})/\|\mathbf{p}_0\|_{L^2} = a$, which is equivalent to $(1 - a^2)\|\mathbf{p}_0\|_{L^2}^2 = \|\boldsymbol{\pi}\|_{L^2}^2$. The programming is now: find A_{min} such that

$$\begin{aligned} A_{min} &= \min_{\boldsymbol{\pi}} A_0(\boldsymbol{\pi}) \\ \boldsymbol{\pi}^* \cdot \mathbf{p}_0 &= \|\boldsymbol{\pi}\|_{L^2}^2 \\ (1 - a^2)\|\mathbf{p}_0\|_{L^2}^2 &= \|\boldsymbol{\pi}\|_{L^2}^2. \end{aligned} \quad (12)$$

To find $A_{min} = \min_{\boldsymbol{\pi}} A_0(\boldsymbol{\pi})$ is equivalent to finding $\max_{\boldsymbol{\pi}} \boldsymbol{\pi}^* \cdot \mathcal{K} \cdot \boldsymbol{\pi}$ or $\min_{\boldsymbol{\pi}} \boldsymbol{\pi}^* \cdot \mathcal{A} \cdot \boldsymbol{\pi}$.

3.2. METHOD FOR FINDING THE SOLUTION

The projection matrix \mathcal{A} is factorized by its eigenvectors and eigenvalues which are 1 or 0. With \mathcal{U} the matrix filled with the eigenvectors, and $\boldsymbol{\Lambda}$ the diagonal matrix of the eigenvalues, one has $\mathcal{A} = \mathcal{U} \cdot \boldsymbol{\Lambda} \cdot \mathcal{U}^*$. The eigenvectors have been normalized in order to obtain $\mathcal{U}^* \cdot \mathcal{U} = \mathbf{I}$. Now upon expressing the pressure vector field $\boldsymbol{\pi}$ on the new base that is, writing $\boldsymbol{\chi} = \mathcal{U}^* \cdot \boldsymbol{\pi}$, as well as $\hat{\mathbf{p}}_0 = \mathcal{U}^* \cdot \mathbf{p}_0$, the programming is

$$\min_{\boldsymbol{\chi}} \boldsymbol{\chi}^* \cdot \boldsymbol{\Lambda} \cdot \boldsymbol{\chi} = \min_{\chi_i} \sum_{i=1}^{N_x} \lambda_i |\chi_i|^2, \quad \text{where } \lambda_i \text{ are 0 or 1,}$$

a quantity which does not depend on the phases of the components of vector $\boldsymbol{\chi}$,

$$\begin{aligned} -\sum_i \bar{\chi}_i \cdot \hat{p}_{0i} + \sum_i |\chi_i|^2 &= 0 = h_1(\boldsymbol{\chi}), \\ -\sum_i \bar{\chi}_i \cdot \hat{p}_{0i} + \sum_i (1 - a^2)\|\mathbf{p}_0\|^2 &= 0 = h_2(\boldsymbol{\chi}). \end{aligned} \quad (13)$$

As the quantity, of which the minimum is being sought, will not depend on the phases of the components of vector $\boldsymbol{\chi}$, one can take the liberty of choosing arbitrarily in the calculations, and for the sake of simplicity, the components of $\boldsymbol{\chi}$ in phase with those of $\hat{\mathbf{p}}_0$ and moreover in the real field, resulting in

$$\begin{aligned} \min_{\chi_i} \sum_i \lambda_i \chi_i^2 &= \min_{\chi} f(\boldsymbol{\chi}), \quad \text{i.e.} \quad \min_{\chi_i} \sum_{i, \text{ for } \lambda_i=1} \chi_i^2 \\ -\sum_i \chi_i \cdot \hat{p}_{0i} + \sum_i \chi_i^2 &= 0 = h_1(\boldsymbol{\chi}), \\ -\sum_i \chi_i \cdot \hat{p}_{0i} + \sum_i (1 - a^2)\|\mathbf{p}_0\|^2 &= 0 = h_2(\boldsymbol{\chi}). \end{aligned} \quad (14)$$

The minimization of this convex problem subjected to equality constraints is carried out by the method of Kuhn–Tucker. It consists in looking for the saddle point of the function, called the Lagrangian, $L(\boldsymbol{\chi}, l_1, l_2) = f(\boldsymbol{\chi}) + l_1 h_1(\boldsymbol{\chi}) + l_2 h_2(\boldsymbol{\chi})$. At the solution, the following equalities are satisfied:

$$\begin{aligned} \nabla_{\boldsymbol{\chi}} f(\boldsymbol{\chi}) + l_1 \nabla_{\boldsymbol{\chi}} h_1(\boldsymbol{\chi}) + l_2 \nabla_{\boldsymbol{\chi}} h_2(\boldsymbol{\chi}) &= 0 \\ h_1(\boldsymbol{\chi}) &= 0, \quad h_2(\boldsymbol{\chi}) = 0. \end{aligned} \quad (15a, b, c)$$

It results from equation (15a) that $\chi_i = [(l_1 + l_2)]/[2(\lambda_i + l_1)] \hat{p}_{0i}$, with λ_i of 0 or 1 value. The expression for l_1 and l_2 derive from equations (15b) and (15c) worked simultaneously with the use of the following fundamental equalities:

$$\begin{aligned} R_0 \|\mathbf{p}_0\|_{L^2}^2 &= \|\mathbf{p}_0\|_{\mathcal{A}}^2 = \mathbf{p}_0^* \cdot \mathcal{A} \cdot \mathbf{p}_0 = \hat{\mathbf{p}}_0^* \cdot \boldsymbol{\Lambda} \cdot \hat{\mathbf{p}}_0 \\ &= \sum_{i, \text{ for } \lambda_i = 1} (\hat{p}_{0i})^2 \text{ when the components are real,} \\ (1 - R_0) \|\mathbf{p}_0\|_{L^2}^2 &= \|\mathbf{p}_0\|_{\mathcal{K}}^2 = \mathbf{p}_0^* \cdot \mathcal{K} \cdot \mathbf{p}_0 = \hat{\mathbf{p}}_0^* \cdot (\mathbf{I} - \boldsymbol{\Lambda}) \cdot \hat{\mathbf{p}}_0 \\ &= \sum_{i, \text{ for } \lambda_i = 0} (\hat{p}_{0i})^2 \text{ when the components are real.} \end{aligned}$$

Apart from this information, the calculation is not of any interest and is not given here. After having obtained the expressions for l_1 and l_2 , the expression for χ_i is deduced.

3.3. CLOSED FORM AND GRAPHS

The expressions for χ_i are now

$$\begin{aligned} \text{for } \lambda_i = 0, \quad \chi_i &= \frac{\sqrt{(1 - a^2)R_0(1 - R_0)} - aR_0}{2\sqrt{(1 - a^2)R_0(1 - R_0)}} (1 - a^2)\hat{p}_{0i}, \\ \text{for } \lambda_i = 1, \quad \chi_i &= \frac{\sqrt{(1 - a^2)R_0(1 - R_0)} - a(1 - R_0)}{2\sqrt{(1 - a^2)R_0(1 - R_0)}} (1 - a^2)\hat{p}_{0i}. \end{aligned}$$

At this point, the result is

$$\begin{aligned} \min_{\chi_i} \sum_{i, \text{ for } \lambda_i = 1} \chi_i^2 &= \left[\frac{\sqrt{(1 - a^2)R_0(1 - R_0)} - a(1 - R_0)}{\sqrt{(1 - a^2)R_0(1 - R_0)}} (1 - a^2) \right] \\ &\times \sum_{i, \text{ for } \lambda_i = 1} \hat{p}_{0i}^2 = (\boldsymbol{\pi}^* \cdot \mathcal{A} \cdot \boldsymbol{\pi})_{\min}. \end{aligned}$$

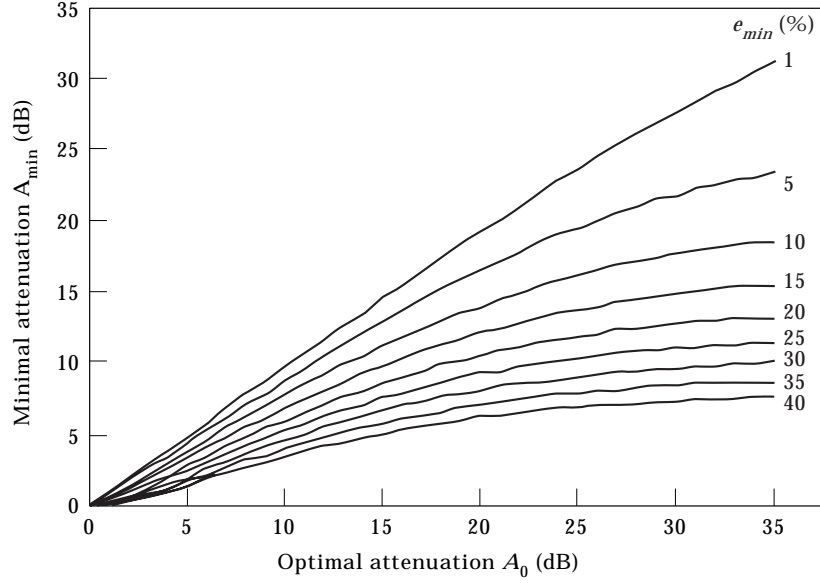


Figure 6. Calculated minimum attenuation versus optimal attenuation for various values of e_{min} .

In view of the constraint $(1 - a^2)\|\mathbf{p}_0\|_{L^2}^2 = \|\boldsymbol{\pi}\|_{L^2}^2$, the minimum attenuation has the final closed form

$$\begin{aligned}
 A_{min} &= -10 \log_{10} \left(1 - \frac{(\boldsymbol{\pi}^* \cdot \mathcal{A} \cdot \boldsymbol{\pi})_{min}}{\|\boldsymbol{\pi}\|_{L^2}^2} \right) \\
 &= -10 \log_{10} (1 - R_0 + a^2(2R_0 - 1) + 2a\sqrt{(1 - a^2)R_0(1 - R_0)}). \quad (16)
 \end{aligned}$$

Note that, were one seeking $\max_{\boldsymbol{\pi}} \boldsymbol{\pi}^* \cdot \mathcal{A} \cdot \boldsymbol{\pi}$, the work would have been carried out with

$$\max_{\lambda_i} \sum_i (1 - \lambda_i \chi_i^2),$$

i.e.,

$$\max_{\lambda_i} \sum_{i, \text{ for } \lambda_i = 0} \chi_i^2,$$

and upon inserting the values of χ_i when $\lambda_i = 0$, the same expression of the minimum attenuation would have been found.

It is now clear that the minimum attenuation depends solely on the reference situation through R_0 and on the error in the spatial distribution of the primary field $a = e_{min}$. The graphs of the minimum attenuation versus the optimal attenuation with the primary field of reference are drawn in Figure 6. This figure has the same meaning as Figure 5 and the reader should refer to the explanations given at that stage. However, unlike Figure 5, Figure 6 is derived from a demonstration.

It should be noted that, at a given value of R_0 , $A_{min}(e_{min})$ decreases to 0 dB while e_{min} goes from 0 to $\sqrt{R_0}$. For a physical system of control submitted to primary field spatial variations of less than $\sqrt{R_0}$, the minimal guaranteed attenuation could be written as

$$A_{min} = -10 \log_{10} (1 - R_0 + a^2(2R_0 - 1) + 2a\sqrt{(1 - a^2)R_0(1 - R_0)}) \quad \text{for } a = e_{min} < \sqrt{R_0},$$

$$A_{min} = 0 \quad \text{for } a = e_{min} \geq \sqrt{R_0}.$$

4. CONTROL SIMULATIONS BY ELEMENTARY EXPERIMENTS

4.1. OBJECTIVE AND MEASUREMENT PROTOCOL

It has previously been seen that the better the optimal attenuation in the reference situation, the better the minimum guaranteed attenuation in the presence of primary field variations. To what extent it is possible to check experimentally what has now been demonstrated theoretically?

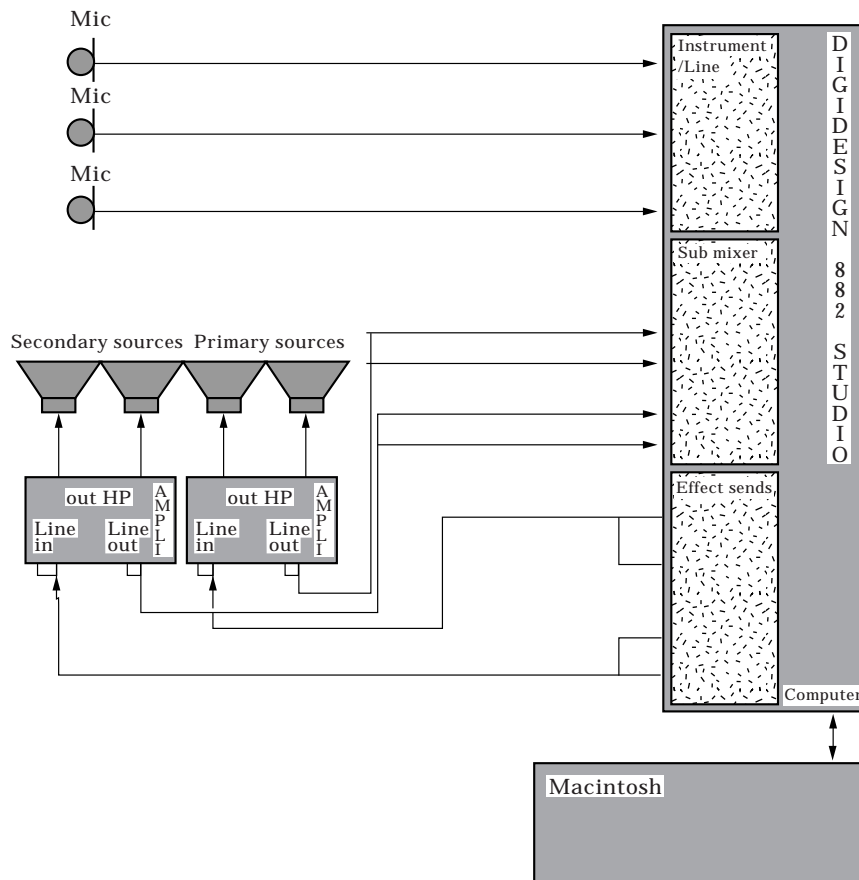


Figure 7. Global diagram of the control system used.

The present experiments in rooms try to isolate the problem of non-stationarity in the spatial distribution of the primary field from among numerous other problems. That is why it is intended momentarily to avoid all the problems that could arise from real time processing in order to find the optimal driving signals by means of the well-known LMS algorithms, for example. Instead, for the time being, the work is carried out in deferred time to avoid algorithmic aspects.

The elementary active noise control experiments were done with two Brüel and Kjaer microphones (free field, half-inch), two loudspeakers and a data processing system made up of recording hardwares Digidesign and Matlab installed on a Macintosh Quadra 650.

The Digidesign multitrack software-hardware has A/D and D/A interfaces and a clock which allows sampled signal to be recorded and sent at 44.1 kHz on 16 bits. Both the microphones and the loudspeakers are linked to the computer through the Digidesign set. Figure 7 shows a more general installation with the system.

The first step in the procedure consists of recording the primary and the secondary fields at the microphones.

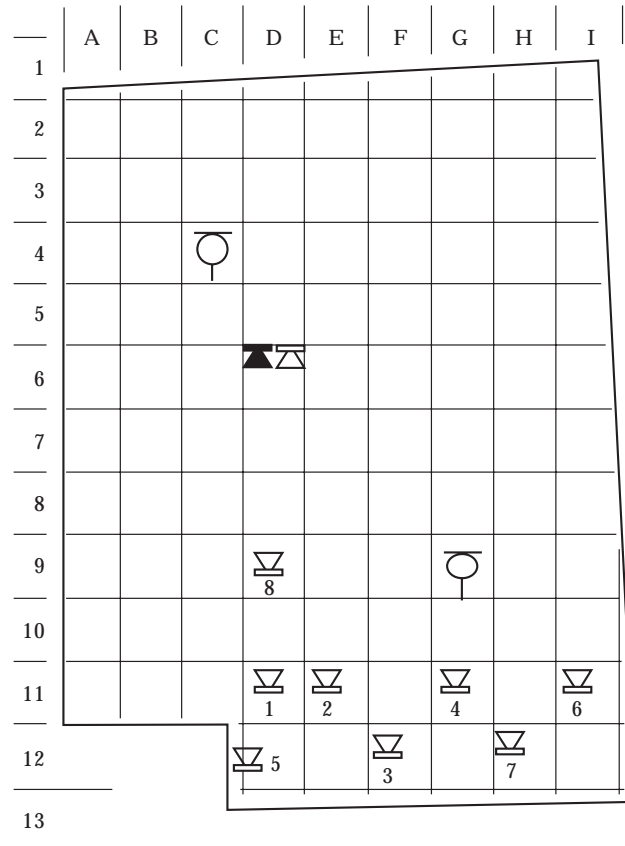
Matlab is then used to determine the optimal driving signal and to predict the optimal attenuation. Before doing this, the frequency, amplitude and phase need to be obtained. From the temporal signal, the frequency is deduced from the zero value detection of the signal (with the great advantage of remaining independent of the recording duration, contrary to a FFT procedure; e.g., the reader probably knows that with a recording duration of 100 ms, the FFT provides the frequency with an error of ± 5 Hz). The calculation of the optimal driving signal in the frequency domain is obtained both by the direct method ($\phi_0 = -\mathbf{H}^{-1} \cdot \mathbf{G}^* \cdot \mathbf{p}_0$) and by the iterative method (gradient method) to be sure of the result.

The third step is to build the temporal signal of the optimal driving control. The fact that the experiment is not carried out in real time leads to particular attention being paid to respect the phase relation between primary and secondary signals. Moreover the duration of the signals must be sufficiently long for the transitory signal to be short with regard to the recording, and to enable the optimal attenuation to be checked.

Finally the simultaneous radiation of the primary and secondary signals provides the residual sound level and thus the experimental optimal attenuation.

The measurement protocol is as follows.

- (1) Locate the primary source at its reference location.
- (2) Seek locations of high primary level in the reference situation since low sound level locations are not going to show a great reduction; the locations were chosen here by ear.
- (3) Locate the secondary source for the configuration i of the control.
- (4) Record the primary and secondary signals.
- (5) Calculate the optimal driving signal and attenuation.
- (6) Simulate the experimental control and obtain the experimental attenuation.
- (7) Modify the primary field by moving the primary source and repeat steps 4 to 6.



∇ : Secondary source locations.

▾ : Primary source locations.

Figure 8. Geometrical configurations for the control.

(8) Calculate e , e_{min} and A_{min} [from equation (16)] as well as $(\delta A)_{max}$ associated with the Taylor series at the first order; check (a) that the minimum attenuation is a lower bound of the optimal attenuation; and (b) that, in the case of first order Taylor series validity, the attenuation is indeed situated between $A_0 - (\delta A)_{max}$ and $A_0 + (\delta A)_{max}$.

(9) Repeat steps 3 to 9 for each envisaged secondary source configuration (here secondary source location).

4.2. IMPLEMENTATION OF ELEMENTARY EXPERIMENTS AND EXPERIMENTAL RESULTS

With a sole secondary source, the only way to modify the spatial distribution of the primary field consists in moving its location. Indeed, given the frequency, the change in the driving signal does not change the spatial distribution of the radiated pressure.

Moreover, it has been observed experimentally that the change in the secondary source location affects the response of the room, especially in reverberant rooms.

This type of problem will always be present in real situations as it will never be envisaged to locate a large number of secondary sources in a cavity to work finally with only a chosen one or few. It results in the impossibility, rigorously speaking, of dealing with the choice of a secondary source configuration with a constant value of relative error in the primary field and zero variation in the response functions of the room.

Nevertheless, the experiment was carried out at 125 Hz in an empty classroom of comfortable volume (120 m^3) and relatively reverberant as the walls were bare. The physical control configuration was minimal in the sense that one source played the role of the primary source, the other was the secondary source, and there were only two control microphones. It should be noted that the reverberation and the small number of sensors will accentuate the effects of the variation in the primary source location which is to induce the primary field variation (see Figure 8).

The implementation of the protocol provided the results in Table 1 and the graph in Figure 9 which show the attenuations in dB against the number of the secondary source location. These locations 1 to 8 correspond to decreasing optimal attenuation in the reference situation.

The relatively good agreement between calculated and measured optimal attenuation in the reference situation is an indicator of the linearity which is fundamental to define a control system. The slight difference is probably due to the non-synchronicity between the recording of the response functions and the primary field, and the experimental verification of the control originating, among others, from the fluctuations in the loudspeakers' electrodynamic behaviors.

The optimal attenuation for the primary field $\mathbf{p}_0 + \delta\mathbf{p}_0$ is always greater than the calculated A_{min} , to within measurement error estimated at 1 dB (for location no. 1 of the secondary source).

Moreover, the minimum attenuation increases with the reference attenuation. It seems that we remain experimentally in zone (b) of Figure 3, i.e., where the first order Taylor series could be used: e.g., the secondary source located at position 2 leads to a reference attenuation of about 15 dB and e_{min} has the value of around 16%, and the point (15 dB, 16%) is to be found in zone 3(b) of Figure 3. In these conditions, with considerations originating from the first order Taylor series only, the width of the error corridor, which comes from the gap between the minimum and the maximum attenuations, remains large except for very poor reference attenuations. In other words, the values of e or the minimization to obtain e_{min} from a measured variation of $\delta\mathbf{p}_0$ —minimization which is really efficient as it leads to around half the value of e (see Table 1), leading also to a significant reduction in the upper bound $(\delta A)_{max}$ of δA —have never been sufficiently small to provide a narrow error corridor for good reference attenuations.

Another experiment was carried out in a different room (400 m^3), relatively damped acoustically, at a slightly different frequency. This other room of large dimensions, with absorptive material on the walls and of complex geometry preventing multiple modes and systems of stationary waves, presents some characteristics of indefinite space. It resulted in very small primary field variations

TABLE 1
 Comparison between theoretical and experimental results for the room of 120 m³ (each configuration of secondary source is associated to one value of e_{min})

Secondary actuator locations	1	2	3	4	5	6	7	8
Theo. $A_0(\mathbf{p}_0)$	19.7	14.9	10.2	8.4	6.1	4.1	4.0	3.7
Exp. $A_0(\mathbf{p}_0)$	19.0	15.6	10.1	6.8	6.1	4.1	4.0	3.0
Theo. $A_0(\mathbf{p}_0 + \delta\mathbf{p}_0)$	11.8	20.1	9.1	5.0	5.2	5.7	2.5	2.5
Exp. $A_0(\mathbf{p}_0 + \delta\mathbf{p}_0)$	12.0	19.9	8.6	4.6	5.3	5.6	2.3	2.5
$(\delta A)_{max}$ (Taylor)	10.6	7.8	4.0	3.8	2.1	1.7	2.2	1.9
Measured δA	7	4.3	1.5	2.2	0.8	1.5	1.7	0.5
$(A_0 + (\delta A)_{max})(\mathbf{p}_0)$ (Taylor)	30.3	22.7	14.2	12.3	8.2	5.8	6.2	5.6
$(A_0 - (\delta A)_{max})(\mathbf{p}_0)$ (Taylor)	9.1	7.1	6.2	4.6	4.0	2.5	1.8	1.8
e	0.2886	0.3113	0.3062	0.3874	0.2666	0.3061	0.2985	0.3318
e_{min}	0.1268	0.165	0.1493	0.1795	0.1397	0.1513	0.2094	0.1876
Theo. A_{min} (from equation (16))	12.8	9.4	7.0	5.4	4.3	2.7	2.2	2.1

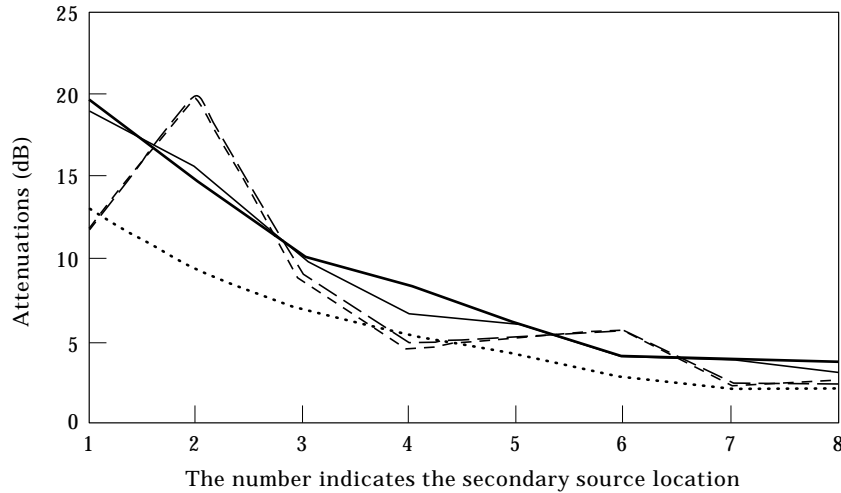


Figure 9. Results of Table 1 presented as a graph: comparison between calculated and measured optimal attenuation in the reference situation and same comparison for another primary field; in the latter case, the results are above the calculated minimum attenuation. —, $A_0(\mathbf{p}_0)$ theo.; —, $A_0(\mathbf{p}_0)$ exp.; —, $A_0(\mathbf{p}_0 + \delta \mathbf{p}_0)$ theo.; —, $A_0(\mathbf{p}_0 + \delta \mathbf{p}_0)$ exp.; \cdots , A_{min} .

(around 4%) compared to those obtained previously with the same order of magnitude in the primary source displacements. It also resulted in difficulties to obtain significant reference attenuations because the characteristics of indefinite acoustic space are not appropriate to control two microphones with one secondary source unless these sensors are on the same wavefront. The results presented were obtained by positioning the microphones near each other.

The same protocol provided the results in Table 2 and the graph in Figure 10 which have to be read like Table 1 and Figure 9.

Again, the optimal attenuation is always greater than the minimum one obtained from equation (16).

Here also, the minimum attenuation increases with the reference attenuation and the configurations are in part 3(b) of Figure 3. This time the width of the error corridor, reachable by considering only the first order Taylor series, is narrow due to the very small primary field variations, and the discrepancy between calculated and measured reference attenuations is of the same order of magnitude as the variations of attenuations originating from the variations of the primary field. Despite this fact, the experimental results always are inside the error corridor.

In the preceding experiments, the modification of the spatial distribution of the primary field was obtained by moving the primary source. It appeared that the minimized relative variation e_{min} of the primary field was highly sensitive to the primary source location and only one reasonable value of the relative variation was worked on. Thus, for each configuration of the secondary source (i.e., its location as long as there exists only one control-source), only one value of e_{min} was considered.

In a third experiment, carried out in a third room of approximately 40 m^3 , the primary field was radiated by two primary sources at the output of a stereophonic amplifier. The spatial modification of the primary field resulted from modifying

TABLE 2
 Comparison between theoretical and experimental results for the room of 400 m³ (each configuration of secondary source is associated to one value of e_{min})

Secondary actuator locations	1	2	3	4	5	6	7	8
Theo. $A_0(\mathbf{p}_0)$	15.5	14.4	13.4	12.2	9.3	9.1	8.9	7.7
Exp. $A_0(\mathbf{p}_0)$	14.8	14.2	12.6	11.0	8.9	9.3	9.1	8.0
Theo. $A_0(\mathbf{p}_0 + \delta\mathbf{p}_0)$	14.6	13.6	13.6	11.4	8.8	9.2	8.7	7.9
Exp. $A_0(\mathbf{p}_0 + \delta\mathbf{p}_0)$	15.1	13.4	13.2	11.5	9.1	9.4	8.9	8.2
$(\delta A)_{max}$ (Taylor)	1.0	1.0	1.4	1.2	0.7	0.5	0.2	0.4
Measured δA	0.3	0.8	0.6	0.5	0.2	0.1	0.2	0.2
$(A_0 + (\delta A)_{max})(\mathbf{p}_0)$ (Taylor)	16.5	15.4	14.8	13.5	10.1	9.6	9.1	8.1
$(A_0 - (\delta A)_{max})(\mathbf{p}_0)$ (Taylor)	14.6	13.4	11.9	11.0	8.6	8.7	8.7	7.2
e	0.0227	0.0282	6.6912	0.6764	0.4638	0.0264	0.0295	0.0526
e_{min}	0.0189	0.023	0.0364	0.0359	0.0305	0.0195	0.0088	0.0229
Theo. A_{min} (from equation (16))	14.6	13.4	12.0	11.1	8.6	8.7	8.7	7.2

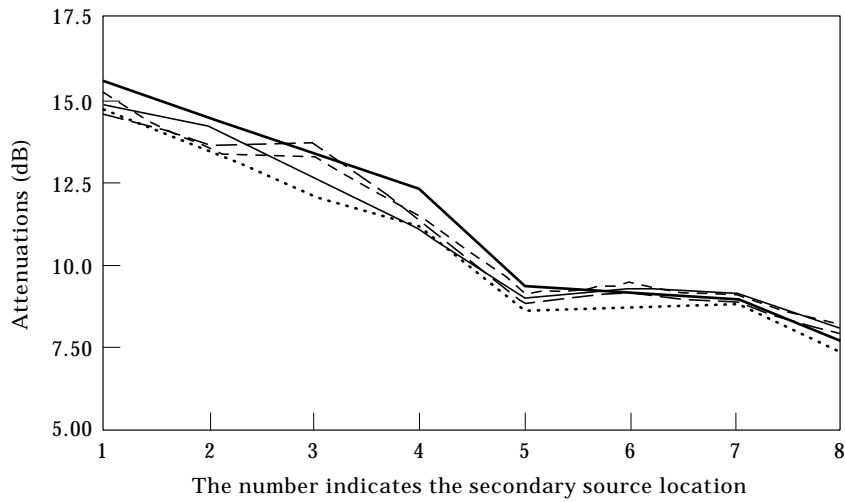


Figure 10. Results of Table 2 presented as a graph: comparison between calculated and measured optimal attenuation in the reference situation and same comparison for another primary field; in the latter case, the results are above the calculated minimum attenuation. Key as Figure 9.

the balance of the amplifier. It appeared that the values of e_{min} vary slowly with the balance, leading to a much better mastery of e_{min} . With this new procedure, Table 3 shows the calculated and measured optimal attenuations accompanying the reference situation as well as those obtained when the primary field varies

TABLE 3

Comparison between theoretical and experimental results for the room of 40 m³ (each configuration of two secondary sources is associated with various values of e_{min})

<i>Secondary actuator locations no. 1</i>								
e_{min} %	0	9	13	19	21	27	39	56
Theo. A_0	13.7	10.9	13.3	14.6	23.4	6.9	4.8	2.4
Exp. A_0	11	9.3	12.1	14	21.2	6	4.2	3.1
A_{min}		8.7	7.9	6.8	6.4	5.5	4.0	2.3
<i>Secondary actuator locations no. 2</i>								
e_{min} %	0	6	24	25	34	37	91	99
Theo. A_0	6.8	6.4	4	3.8	3.8	9.1	2	1.3
Exp. A_0	5.7	5.5	3.2	3.3	4.3	8.7	1.7	2.1
A_{min}		4.9	3.0	2.9	2.2	2.0	0.0	0.0
<i>Secondary actuator locations no. 3</i>								
e_{min} %	0	7	8	11	12	27	39	53
Theo. A_0	4.2	4.7	4.6	4.5	4.4	5.5	6.24	4.2
Exp. A_0	3.6	3.8	3.5	5	4	4.9	6.5	3.9
A_{min}		3.0	2.9	2.6	2.5	1.5	0.9	0.4
<i>Secondary actuator locations no. 4</i>								
e_{min} %	0	6	7	9	13	26	27	28
Theo. A_0	12.2	14.6	13.4	9.6	8.6	10.3	10.2	7.2
Exp. A_0	11.7	13.8	12.3	10.1	9	10.1	9.1	6.5
A_{min}		10.0	9.7	9.2	8.3	6.0	5.8	5.7

around its reference value. These variations are characterized by e_{min} and $A_{min}(A_0, e_{min})$, obtained from the curves of Figure 6. It is observed that, on the one hand, the value of A_{min} is always a value by default, and on the other, $\forall e_{min} \leq e_{min}^{max}$ (the greatest value of e_{min} associated to a given primary field), that $A_0(\mathbf{p}_0 + \delta\mathbf{p}_0)$ is always greater than $A_{min}(A_0(\mathbf{p}_0), e_{min}^{max})$. For example, the first table obtained from a configuration of three microphones and two control-sources indicates $e_{min}^{max} = 56\%$ and $A_{min}(A_0 = 13.7 \text{ dB}, e_{min}^{max} = 56\%)$ is 2.3 dB; $\forall e_{min} < 56\%$, it appears that $A_0(\mathbf{p}_0 + \delta\mathbf{p}_0)$ is always greater than 2.3 dB.

5. SUMMARY AND CONCLUSION

The harmonic sound level attenuations achieved in vehicles by means of the active noise control technique differ greatly according to the way they have been obtained, by numerical modelling or by *in situ* experiments. From among the reasons at the origin of the optimism of numerical results, the one concerning the perfect stationarity of the primary sound field spatial distribution in the models, which does not exist in the real world, has been examined here in depth. Thus the paper has been focused on variation in attenuation according to the spatial stationarity error, emphasizing the minimum attenuation that a model can guarantee while taking into consideration this error.

The Taylor series, at the first order, of the optimal attenuation seen as a function of the primary field, and the minimization of its relative error, are the first steps taken in the theoretical approach. If this approach had been realistic, it would have shown that, for a given spatial stationarity error, the minimum guaranteed attenuation would not always have been an increasing function of the optimal attenuation which accompanies the primary field of the reference situation, as it decreases after having reached a maximum value. Such a variation would have destroyed the secondary source configurations classification according to efficiency in the reference situation.

Thanks to very simple calculations, the validity domain of the approximated theoretical approach has been drastically bounded. It has been observed that the minimal attenuation begins its variation according to the optimal attenuation by increasing, but then almost reaches a maximum value while the optimal attenuation continues to increase. For example, for a stationarity error of 10%, the minimal attenuation reaches 12 dB when the optimal attenuation is 16 dB, and then the minimum attenuation increases by scarcely 5 dB while the optimal attenuation increases to 40 dB.

All the information gathered at this stage has influenced the way the problem is now posed and solved, to end with the closed form of the minimum attenuation which clarifies all the previous approaches. The calculations carried out to solve the problem rest on the projection operators, the Kuhn–Tucker method and the Lagrange multipliers accessible analytically.

As to the experimental part of the study, very simple experiments were carried out which show that the real attenuation remains above the minimum attenuation.

The very new information presented in this paper is fundamental for the prediction of active control of sound in the frequency domain. Indeed above a certain degree of optimal attenuation, the minimum guaranteed attenuation is

almost saturated. It is time now to mention that, for active control in the passengers' cabin of aircraft, it is quite common to obtain up to 30 dB of optimal attenuation [4], while the attenuation observed in the real world rarely reaches more than 15 dB [8–11]. If the only error had been that of the spatial stationarity, it would have been around 15% and it is not relevant to look for more than 20 dB of optimal attenuation. Within the present context, the goal is, more adequately, to attain 20 dB with the smallest possible number of secondary sources, in order to guarantee 13 dB.

From the scientific point of view, it is worth emphasizing the progression towards the final information: reflection on an approximate theoretical formulation showing the importance of variables R_0 , e and e_{min} ; the implementation of a very simple numerical simulation with the previous variables leading to the independence of A_{min} from the configuration of the physical system of control; the creation of the demonstration to achieve the closed form of A_{min} , originating from the information obtained previously; the implementation of elementary experimental verifications.

REFERENCES

1. E. BENZARIA and V. MARTIN 1995 in *The 1995 International Symposium on Active Control of Sound and Vibration, Institute of Noise Control Engineering of the U.S.A.*; New York; Noise Control Foundation. Constrained optimization of secondary source locations in ANC: multipolar arrangements of sources. 499–510.
2. K. H. BAEK and S. J. ELLIOTT 1995 *Journal of Sound and Vibration* **186**(2), 245–267. Natural algorithms for choosing source locations in active control systems.
3. B. NAYROLES, G. TOUZOT and P. VILLON 1994 *Journal of Sound and Vibration* **171**(1), 1–21. Using diffuse approximation for optimizing the locations of antisound sources.
4. V. MARTIN, PH. VIGNASSA and B. PESEUX 1994 *Journal of Sound and Vibration* **176**(3), 307–332. Numerical vibro-acoustic modelling of aircraft for the active acoustic control of interior noise.
5. G. M. L. GLADWELL and G. ZIMMERMANN 1966 *Journal of Sound and Vibration* **3**, 233–241. On energy and complementary energy formulations of acoustic and structural vibration problems.
6. V. MARTIN and C. CARIU 1997 in *The 1997 International Symposium on Active Control of Sound and Vibration, organized by Scientific Society for Optics, Acoustics, Motion Pictures and Theater Technology (OPAKFI), Budapest, Hungary*. Harmonic sound field active attenuation improved by modifying the primary field. 673–688.
7. F. DAHAN 1996 *Thèse de doctorat, Université d'Aix-Marseille II*. Qualification d'un système physique de contrôle acoustique structural actif.
8. A. SOLLO, J. FITZPATRICK, V. MARTIN and G. VENET 1993 *Aerodays 93, Naples*. Theoretical and experimental results of Asanca study for ATR 42 application.
9. S. J. ELLIOTT, P. A. NELSON, I. STOTHERS and C. BOUCHER 1989 *Journal of Sound and Vibration* **128**(2), 355–357. Preliminary results of in-flight experiments on the active control of propeller-induced cabin noise.
10. C. M. DORLING, G. P. EATWELL, S. M. HUTCHINS, C. F. ROSS and S. G. C. SUTCLIFFE 1989 *Journal of Sound and Vibration* **128**(2), 358–360. A demonstration of active noise reduction in an aircraft cabin.
11. S. J. ELLIOTT, P. A. NELSON, I. STOTHERS and C. BOUCHER 1990 *Journal of Sound and Vibration* **140**(2), 210–238. In-flight experiments on the active control of propeller-induced cabin noise.